

# 1 **Glacier melting and precipitation trends detected by surface area** 2 **changes in Himalayan ponds**

3 Franco Salerno<sup>(1,3)</sup>, Sudeep Thakuri<sup>(1,3)</sup>, Nicolas Guyennon<sup>(2)</sup>, Gaetano Viviano<sup>(1)</sup>, Gianni Tartari<sup>(1,3)</sup>

4 <sup>(1)</sup> National Research Council, Water Research Institute, Brugherio (IRSA-CNR), Italy

5 <sup>(2)</sup> National Research Council, Water Research Institute, Roma (IRSA-CNR), Italy

6 <sup>(3)</sup> Ev-K2-CNR Committee, Via San Bernardino, 145, Bergamo 24126, Italy

7 *Correspondence to Franco Salerno (salerno@irsa.cnr.it)*

8 **Abstract.** Climatic time series for high-elevation Himalayan regions are decidedly scarce. Although  
9 glacier shrinkage is now sufficiently well described, the changes in precipitation and temperature at these  
10 elevations are less clear. This contribution shows that the surface area variations of unconnected glacial  
11 ponds, i.e., ponds not directly connected to glacier ice, but that may have a glacier located in their  
12 hydrological basin, can be considered as suitable proxies for detecting past changes in the main  
13 hydrological components of the water balance. On the south side of Mt. Everest, glacier melt and  
14 precipitation have been found to be the main drivers of unconnected pond surface area changes (detected  
15 mainly with Landsat imagery). In general, unconnected ponds have decreased significantly by  
16 approximately 10±5% in terms of surface area over the last fifty years (1963-2013 period) in the study  
17 region. Here, an increase in precipitation occurred until the mid-1990s followed by a decrease until  
18 recent years. Until the 1990s, glacier melt was constant. An increase occurred in the early 2000s, while a  
19 declining trend in maximum temperature has caused a reduction in the glacier melt during the recent  
20 years.

## 21 **1 Introduction**

22 Meteorological measurements in high-elevation Himalayan regions are scarce due to the harsh  
23 conditions of these environments and their remoteness, which limit the suitable maintenance of weather  
24 stations (e.g., Vuille, 2011; Salerno et al., 2015). Consequently, the availability of long series is even more  
25 rare (Barry, 2012; Rangwala and Miller, 2012; Pepin et al., 2015). Generally, gridded and reanalysis  
26 meteorological data are used to overcome this lack of data and can be considered an alternative (e.g., Yao  
27 et al., 2012). However, in these remote environments their use for climate change impact studies at the  
28 synoptic scale must be performed with caution due to the absence of weather stations across the overall  
29 region, which limits the ability to perform land-based evaluations of these products (e.g., Xie et al., 2007).  
30 Consequently, the meager knowledge on how the climate has changed in recent decades in high-elevation  
31 Himalayan regions presents a serious challenge to interpreting the relationships between causes and  
32 recently observed effects on the cryosphere. Although glacier reduction in the Himalaya is now  
33 sufficiently well described (Bolch et al., 2012; Yao et al., 2012, Kääb, et al., 2012), the manner in which  
34 changes in climate drivers (precipitation and temperature) have influenced the shrinkage and melting  
35 processes is less clear (e.g., Bolch et al., 2012; Salerno et al., 2015), and this lack of understanding is  
36 amplified when forecasts are conducted.

37 In this context, the recent literature has already demonstrated the high sensitivity of lakes and ponds to  
38 climate (e.g., Pham et al., 2008; Williamson et al., 2008; Adrian et al., 2009; Lami et al., 2010). Some

39 climate-related signals are highly visible and easily measurable in lakes. For example, climate-driven  
40 fluctuations in lake surface areas have been observed in many remote sites. Smol and Douglas (2007)  
41 reported decadal-scale drying of high Arctic ponds due to changes in the evaporation/precipitation ratio.  
42 Smith et al. (2005), among other authors, found that lakes in areas of discontinuous permafrost in Alaska  
43 and Siberia have disappeared in recent decades. In the Italian Alps, Salerno et al. (2014a) found that since  
44 the 1980s, lower-elevation ponds have experienced surface area reductions due to increased  
45 evaporation/precipitation ratio for the effect of higher temperature, while higher-elevation ponds have  
46 increased in size and new ponds have appeared as a consequence of glacial retreat.

47 In high mountain Asia and in particular in the interior of the Tibetan Plateau, the observed lake growth  
48 since the late 1990s is mainly attributed to increased precipitation and decreased evaporation (Lei et al.,  
49 2014; Song et al., 2015). In contrast, Zhang et al., 2015, attribute the observed increases in lake surface  
50 areas since the 1990s across entire Pamir-Hindu Kush-Karakoram-Himalaya region and the Tibetan  
51 Plateau region to enhanced glacier melting. Wang et al., 2015, reached similar conclusions in a basin  
52 located in the south-central Himalaya. In our opinion, the divergences in the causes leading to the lake  
53 surface area variations in central Asia are due to the fact that different types of glacial lakes (described  
54 below) have been considered in these studies.

55 In general, in high mountain Asia, three types of glacial lakes can be distinguished according to Ageta  
56 et al. (2000) and Salerno et al. (2012): (i) lakes that are not directly connected with glacier ice but that  
57 may have a glacier located in their hydrological basin (unconnected glacial lakes); (ii) supraglacial lakes,  
58 which develop on the surface of a downstream portion of a glacier; and (iii) proglacial lakes, which are  
59 moraine-dammed lakes that are in contact with the glacier front. Some of these lakes store large quantities  
60 of water and are susceptible to glacial lake outburst floods (GLOFs). Factors controlling the growth of  
61 supraglacial lakes depend on the glacier features from which they develop (surface gradient, mass  
62 balance, cumulative surface lowering, and surface velocity) (Reynolds, 2000; Quincey et al., 2007; Sakai  
63 and Fujita, 2010; Salerno et al., 2012; Sakai, 2012, Thakuri et al., 2015). The causes of proglacial lake  
64 development are decidedly similar to those described for supraglacial lakes(e.g., Bolch et al., 2008;  
65 Salerno et al., 2012; Thakuri et al., 2015). Their filling and drainage is linked to the supply of meltwater  
66 from snow or glacial sources (Benn et al., 2001; Liu et al., 2015). Therefore, the lake  
67 unconnected glacial lakes do not have a close dependence on glacier dynamic and this aspect makes  
68 them potential indicators of the water balance components in high-elevation lake basins i.e., precipitation,  
69 glacier melting, and evaporation. These main contributions would best explain the causes of lake changes  
70 (e.g., Song et al., 2014; Wang et al., 2015, Salerno et al., 2015).A valuable opportunity for a fine-scale  
71 investigation on climate-driven fluctuations in lake surface area is particularly evident on the south slopes  
72 of Mt. Everest (Nepal), which is one of the most heavily glacierized parts of the Himalaya (Scherler et al.,  
73 2011). Additionally, this region has the largest number of lakes in the overall Hindu-Kush-Himalaya  
74 range (Gardelle et al., 2011), and a twenty-year series of temperature and precipitation data has recently  
75 been reconstructed for these high elevations (5000 m a.s.l.) (Salerno et al., 2015). Moreover, the relative  
76 small size of the water bodies in this region, which we can be defined as ponds according to Hamerlik et  
77 al. (2013) (a threshold of  $2 \cdot 10^4 \text{ m}^2$  exists between ponds and lakes), make them especially susceptible to  
78 the effects of climatic changes because of their relatively high surface area to depth ratios (Smol and  
79 Douglas, 2007).This contribution examines the surface area changes of unconnected glacial ponds on the  
80 south side of Mt. Everest (an example is shown in Fig. 1) during the last fifty years (1963-2013). This  
81 study aims to evaluate whether they might be used as proxy to infer past spatial and temporal trends of the  
82 main components of the hydrological cycle (precipitation, glacier melting, and evaporation) at high  
83 elevations. Possible drivers of change are investigated through land climatic data, available in the area,

84 and correlation analysis. Furthermore, morphological boundary conditions (glacier cover, pond size, pond  
85 location, basin aspect, basin elevation) are analysed as possible factors controlling the pond surface area  
86 changes. The study is concluded comparing gridded and reanalysis time series (evaluated vs land climatic  
87 data) with observed pond surface area changes in the last fifty years.

## 88 **2 Region of investigation.**

89 The current study is focused on the southern Koshi (KO) Basin, which is located in the eastern part of  
90 central Himalaya ((Thakuri et al., 2014) (Fig. 2). In particular, the region of investigation is the southern  
91 slopes of Mt. Everest in Sagarmatha (Mt. Everest) National Park (SNP) (27 ° 45' to 28° 7' N; 85° 59' to  
92 86° 31' E) (Fig. 2a) (Amatya et al., 2010; Salerno et al., 2010). The SNP (1148 km<sup>2</sup>) is the highest  
93 protected area in the world, extending from an elevation of 2845 to 8848 m a.s.l. (Salerno et al., 2013).  
94 Land cover classification shows that almost one-third of the territory contains temperate glaciers and less  
95 than 10% is forested (Bajracharya et al., 2010), mainly with *Abies spectabilis* and *Betula utilis* (Bhujju et  
96 al., 2010).

97 The climate is characterized by monsoons, with a prevailing S-N direction (Ichiyanagi et al., 2007).  
98 For the 1994-2013 period at the Pyramid meteorological station (5050 m a.s.l.) (Fig. 2a), the total annual  
99 accumulated precipitation is 446 mm, with a mean annual temperature of -2.45 °C. In total, 90% of the  
100 precipitation falls between June-September. The probability of snowfall during these months is very low  
101 (4%) but reaches 20% at the annual level. Precipitation linearly increases to an elevation of 2500 m and  
102 exponentially decreases at higher elevations (Salerno et al., 2015).

103 Most of the large glaciers in the SNP are debris-covered, i.e., the ablation zone is partially covered with  
104 supraglacial debris (e.g., Scherler et al., 2011; Bolch et al., 2011; Thakuri et al., 2014). However, the  
105 glaciers located within the considered pond basins are very small, steep, clings to the mountain peaks, and  
106 thus they did not develop a debris covered ablation area. The glacier surfaces are distributed from  
107 approximately 4300 m to above 8000 m a.s.l., with more than 75% of the glacier surfaces lying between  
108 5000 m and 6500 m a.s.l. The area-weighted mean elevation of the glaciers is 5720 m a.s.l. in 2011  
109 (Thakuri et al., 2014). Glaciers in this region are identified as summer-accumulation glaciers that are fed  
110 mainly by summer precipitation from the South Asian monsoon system (Ageta and Fujita, 1996). Salerno  
111 et al. (2012) performed the complete inventory of lakes and ponds in the SNP by digitizing ALOS-08  
112 imagery and assigning each body of water a numerical code (LCN, lake cadaster number) according to  
113 Tartari et al. (1998). They reported a total of 624 water bodies in the park, including 17 proglacial ponds,  
114 437 supraglacial ponds, and 170 unconnected ponds. Previous studies revealed that the areas of proglacial  
115 ponds increased on the south slopes of Mt. Everest after the early 1960s (Bolch et al., 2008; Tartari et al.,  
116 2008; Gardelle et al., 2011, Thakuri et al., 2015). Many studies have indicated that the current moraine-  
117 dammed or ice-dammed ponds are the result of coalescence and growth of supraglacial ponds (e.g., Fujita  
118 et al., 2009; Watanabe et al., 2009; Thompson et al., 2012, Salerno et al., 2012). Such ponds pose a  
119 potential threat due to GLOFs. Imja Tsho (Lake) is one of the proglacial lakes in the Everest region that  
120 developed in the early 1960s as small pond and subsequently expanded continuously (Bolch et al., 2008;  
121 Somos-Valenzuela et al., 2014, Fujita et al., 2009; Thakuri et al., 2015).

## 122 **3 Data and Methods**

### 123 **3.1 Overall methodological approach**

124 This section provides a brief description of the overall methodological approach applied in this study.  
125 Whereas in the following sections, data and methods are described in detail.

126 An intra-annual analysis has been carried out throughout the year 2001 on a limited set of

127 unconnected ponds for detecting the months characterized by the lowest surface area intra-annual  
128 variability and consequently the best period of the year to select the satellite images necessary for the  
129 inter-annual analysis.

130 An inter-annual analysis has been carried out during the 2000-2013 period (hereafter we refer to this  
131 analysis as “*short-term inter-annual analysis*”), considering the wide availability of satellite imagery in  
132 this period, on some selected unconnected ponds (hereafter we refer to these ponds as “*selected ponds*”)  
133 to continuously track the inter-annual variations in surface area. This analysis aims to investigate the  
134 possible drivers of change (precipitation, evaporation and glacier melt) considering the availability of  
135 continuous series of annual pond surface areas and climatic data from a land station located in the area.  
136 The study has been carried out through a correlation analysis and a Principal Component Analysis (PCA).

137 An inter-annual analysis has been carried out from 1963 to 2013 (hereafter we refer to this analysis as  
138 “*long-term inter-annual analysis*”) on a wider unconnected pond population (hereafter we refer to this  
139 population as “*all considered ponds*”) and on glaciers located within their hydrological basin. Two kinds  
140 of analyses have been carried out on this set of data: 1) Pond surface area changes have been related to  
141 certain morphological boundary conditions. This analysis allows to investigate the factors controlling the  
142 pond surface area changes. The significance of the observed differences has been evaluated with specific  
143 statistical tests; 2) Pond surface area changes have been related to climatic data. This analysis aims to  
144 point out the capability of unconnected ponds to infer on the detected drivers of change also in the past  
145 when land climatic data did not exist. This study needed a preliminary analysis to reconstruct the climatic  
146 trends before the year 1994. Selected regional gridded and reanalysis datasets have been compared with  
147 land weather data available for the 1994-2013 period.

### 148 3.2 Climatic data

149 The monthly mean of daily maximum, minimum, and mean temperature and monthly cumulated  
150 precipitation time series used in this study have been reconstructed for the elevation of the Pyramid  
151 Laboratory (5050 m a.s.l.) (Fig. 2) for the 1994-2013 period (Salerno et al., 2015). The potential  
152 evaporation for the period (2003-2013) has been calculated by applying the Jensen-Haise model (Jensen  
153 and Haise, 1963) using the mean daily air temperature and daily solar radiation recorded continuously  
154 during the 2003-2013 period at Pyramid Laboratory. The Jensen-Haise model is considered to be one of  
155 the most suitable evaporation estimation methods for high elevations (e.g., Gardelle et al., 2011; Salerno  
156 et al., 2012).

157 To obtain information on climatic trends in the antecedent period (before 1994), we used some  
158 regional gridded and reanalysis datasets. We selected the closest grid point to the location of the Pyramid  
159 Laboratory, and all data were aggregated monthly to allow a comparison at the relevant time scale. With  
160 respect to precipitation, we test the monthly correlation between the Pyramid data and the GPCC (Global  
161 Precipitation Climatology Centre), APHRODITE (Asian Precipitation-Highly Resolved Observational  
162 Data Integration Towards Evaluation of Water Resources), Era-Interim reanalysis of the European Centre  
163 for Medium-Range Weather Forecasts (ECMWF), and CRU (Climate Research Unit Time Series)  
164 datasets. For mean air temperature, we considered the Era-Interim, CRU, GHCN (Global Historical  
165 Climatology Centre), and NCEP-CFS (National Centers for Environmental Prediction Climate Forecast  
166 System) datasets, whereas for maximum and minimum temperatures, we used the Era-Interim and NCEP-  
167 CFS datasets (details on the gridded and reanalysis products are reported in Table SI1).

### 168 3.3 Pond digitization

169 **3.3.1 Long-term inter-annual analysis**

170 Pond surface areas were manually identified and digitized using a topographic map from 1963 and  
171 more recent satellite imagery from 1992 to 2013. The topographic map of the Indian survey of the year  
172 1963 (hereafter TISmap-63, scale 1:50,000) was used to complement the results obtained from the  
173 declassified Corona KH-4 (15 Dec 1962, spatial resolution 8 m). Thakuri et al. (2014) described the co-  
174 registration and rectification procedures applied to the Corona KH-4 imagery. Unfortunately, on these  
175 satellite images many ponds are snow-covered. Therefore here we considered the ponds surface area  
176 digitalized on TISmap-63. The accuracy of this map has been tested comparing the surface areas of 13  
177 ponds digitalized on both data sources (favouring the cloud and shadow free ponds). Figure SI1 shows the  
178 proper correspondence of these comparisons. Furthermore, in order to estimate the mean bias associated  
179 with TISmap-63, we calculated the mean absolute error (MAE) (Willmott and Matsuura, 2005) between  
180 data, which resulted sufficiently low (3.6%), assuring in this way the accuracy of ponds surface area  
181 digitalized on TISmap-63.

182 In total, five scenes were considered according to the availability of satellite imagery. Landsat images  
183 have been mainly used, except in 2008, when in the region the ALOS image, presenting a better  
184 resolution, was available (details on data sources are provided in Table SI2).

185 We tracked only those ponds present continuously in all these five periods to exclude possible  
186 ephemeral water bodies. As described below, 64 ponds have been tracked from 1963 to 2013 (Fig. 2a).

187 **3.3.2 Short-term inter-annual analysis**

188 From the 2000-2013 period, due to a wider availability of satellite imagery (and in particular the  
189 Landsat imagery), 10 ponds were selected among the pond population (64 ponds) considered in the long-  
190 term analysis (1963-2013) to continuously track the inter-annual variations in surface area in the recent  
191 years. The largest ponds, free from cloud cover, and with diverse glacier coverages (from 1% to 32%)  
192 within their hydrological basin were favored in the selection (details on data sources used for these ponds  
193 are provided in Table SI3).

194 **3.3.3 Intra-annual analysis**

195 The intra-annual variability in pond surface area has been investigated throughout the year 2001  
196 through the availability of 5 cloud-free satellite images from June to December (details on data sources  
197 used for these ponds are provided in Table SI4). The first months of the year were excluded from the  
198 analysis because many ponds were frozen until April/May. Even in this case, the main criterion driving  
199 the ponds selection was the absence of cloud cover from the satellite images over the pixels representing  
200 the pond surface area. Only ponds for which a continuous series of data was retrieved from June to  
201 December were selected. Moreover the largest ponds were favored in order to reduce the uncertainty in  
202 the shoreline delineation. Thus, 4 ponds were selected, and their intra-annual variability is tracked in  
203 Figure 3. We observe a common significant increase in pond surface area during the summer months,  
204 likely due to monsoon precipitation and high glacier melting rates. This increase in surface area  
205 disappears on average during the fall. Some single ponds present a dispersion of around 5% between  
206 October and December (LCN4 and LCN77). However, the same Figure points out that just averaging this  
207 information on a population only a little bit larger, the dispersion between October and December  
208 becomes almost zero (1%). Therefore these months are the best period to select the satellite images  
209 necessary for the inter-annual analysis of pond surface area. In fact, during these months, the ponds are

210 not yet frozen, the sky is almost free from cloud cover, and, as observed in Figure 3, the inter-annual  
211 analysis on average is not affected by intra-annual seasonality. Consequently all images for the inter-  
212 annual analysis have been selected from these months (Table SII; Table SI2). Generally, climatic  
213 inferences coming from the analysis of surface area of ponds surely needs to consider a wider number of  
214 ponds in order to reduce the intra-annual variability due to the local conditions of each lake.

### 215 **3.4 Glacier surface areas and melt.**

216 Glacier surface areas within the basins containing the ponds were derived from the Landsat 8 remote  
217 imagery (October 10, 2013) taken by the Operational Land Imager (OLI) with a resolution of 15 m. The  
218 satellite imagery used to track the inter-annual variations in glaciers since the early 1960s is reported in  
219 Table SI2. Detailed information of digitization methods are described in Thakuri et al., 2014.

220 To simulate the daily melting of the glaciers associated with the 10 selected ponds, we used a simple  
221 T-index model (Hock, 2003). This model is able to generate daily melting discharges as a function of  
222 daily air temperature above zero, the glacier elevation bands (using the Digital Elevation Model –DEM-  
223 described below), and a melt factor ( $0.0087 \text{ m d}^{-1} \text{ }^{\circ}\text{C}^{-1}$ ) provided by Kayastha et al. (2000) from a field  
224 study (Glacier AX010) located close to the SNP (southwest). The Glacier AX010 glacier is a small debris  
225 free glacier, located in the Dudh Koshi valley in same climatic and geographic setting of glaciers  
226 considered here. The choice of using a simple model of melting is due to the fact that this paper does not  
227 have the specific objective to provide an accurate evaluation of the magnitude of the melt water released  
228 from glaciers located in the pond basins, but rather to estimate its trend, as function of the temperature, in  
229 order to evaluate if the glacier melt is a possible driver of changes of the pond surface areas. Being  
230 interested in the melt trend and not in its absolute magnitude and considering that these small glaciers are  
231 ungauged, we do not need more sophisticated melt models, which consider specific geometries and  
232 differentiated melt factors.

233 T-index model has been applied here considering the daily temperature of the Pyramid Laboratory  
234 corrected using the monthly lapse rates reported in Salerno et al., 2015 for each 50 m glacier elevation  
235 band. The melt estimated for each band has been then summed to calculate the total melt for each glacier.

### 236 **3.5 Morphometric parameters**

237 The parameters related to the ponds basin as the area, slope, aspect, and elevation were calculated  
238 through the DEM derived from the ASTER GDEM (Tachikawa et al., 2011). ..The vertical and horizontal  
239 accuracy of the GDEM are ~20 m and ~30 m, respectively (Tachikawa et al., 2011; Hengl and Reuter,  
240 2011). We decided to use the ASTER GDEM instead of the Shuttle Radar Topography Mission (SRTM)  
241 DEM considering the higher resolution (30 m and 90 m, respectively) and the large data gaps of the  
242 SRTM DEM in this study area (Bolch et al., 2011). Furthermore, the ASTER GDEM shows better  
243 performance in mountainous terrains (Frey et al., 2012). Hydrological basins have been digitalized using  
244 ArcGIS<sup>®</sup> hydrology tools as carried out by other authors (e.g., Pathak et al., 2013). The circular  
245 statistic has been used for computing the (vector) mean and median values of glaciers and basins aspect  
246 (Fisher, 1993).

### 247 **3.6 Uncertainty of measurements**

248 All of the imagery and map were co-registered in the same coordinate system of WGS 1984 UTM Zone  
249 45N. The Landsat scenes were provided in standard terrain-corrected level (Level 1T) with the use of

250 ground control points (GCPs) and necessary elevation data (LANDSAT SPPA Team, 2015). The ALOS-  
251 08 image used here was orthorectified and corrected for atmospheric effects as described in Salerno et al.  
252 (2012).

253 Concerning the accuracy of the measurements, we refer mainly to the work of Tartari et al.  
254 (2008), Salerno et al. (2012), and Salerno et al. (2014a) which address in detail the problem of  
255 uncertainty in the morphometric measurements related to ponds and glaciers obtained from  
256 remote sensing imagery, maps and photos. The uncertainty in the measurement of a shape's  
257 dimension is dependent both upon the Linear Error (LE) and its perimeter. In particular for  
258 ponds,(as discussed by many authors, only the Linear Resolution Error (LRE) needs to be  
259 considered (e.g., Fujita et al., 2009, Gardelle et al., 2011). Therefore we did not consider the co-  
260 registration error because the comparison was not performed pixel by pixel, at the entity level  
261 (pond) (Salerno et al., 2012, Salerno et al., 2015, Thakuri et al., 2015; Wang et al., 2015). The  
262 LRE is limited by the resolution of the source data. In the specific study of temporal variations  
263 of ponds, Fujita et al. (2009) and Salerno et al. (2012) assumed an error of  $\pm 0.5$  pixels, assuming  
264 that on average the lake margin passes through the centers of pixels along its perimeter. The  
265 uncertainties in the changes in pond surface area were derived using a standard error  
266 propagation rule, i.e., the root sum of the squares (uncertainty =  $\sqrt{e_1^2 + e_2^2}$ ), where  $e_1$  and  $e_2$  are  
267 uncertainties from the first and second scene) of the mapping uncertainty in two scene Salerno  
268 et al., 2012; Thakuri et al., 2015).

### 269 **3.7 Statistical analysis**

270 In the short-term inter-annual analysis, the degree of correlation among the data was verified through  
271 the Pearson correlation coefficient ( $r$ ) after testing that the quantile-quantile plot of model residuals  
272 follows a normal distribution (not shown here) (e.g., Venables and Ripley, 2002). All tests are  
273 implemented in the software R (R Development Core Team, 2008) with the significance level at  $p < 0.05$ .  
274 The normality of the data is tested using the Shapiro–Wilk test (Shapiro and Wilk, 1965; Hervé, 2015).  
275 Razali and Waph, 2011 demonstrate that the Shapiro-Wilk test presents the highest power for small  
276 sample size. The data were also tested for homogeneity of variance with the Levene's test (Fox and  
277 Weisberg, 2011). All comparisons conducted in this study are homoscedastic.

278 To evaluate the significance of differences in surface area changes of ponds population, both in time  
279 and respect certain morphological boundary conditions, some parametric and non-parametric tests have  
280 been used. We applied the paired t-test to compare the means of two normally distributed series. If the  
281 series were not normal, as a non-parametric ANOVA, we used the Friedman test for paired comparisons  
282 and the post-hoc test according to Nemenyi (Pohlert, 2014), while for non-paired comparisons we applied  
283 the Kruskal-Wallis test and the post-hoc test according to Nemenyi-Damico-Wolfe-Dunn (Hothorn et al.,  
284 2015). The significance of the temporal trends has been tested using the Mann Kendall test ( $p < 0.10$ )  
285 (Mann, 1945; Kendall, 1975; Guyennon et al., 2013). When a time series is not very long, the associated  
286 significance level should be considered with caution.

287 We conducted a Principal Component Analysis (PCA) as described in Wold et al. (1987) between pond  
288 surface area variations and climatic variables to obtain information on relationships among the data and to  
289 look for reasons that could justify the observed changes in the pond size (e.g., Settle et al., 2007; Salerno  
290 et al., 2014a,b; Viviano et al., 2014).

## 291 4. Results4.1 Pond and glacier surface area variations

292 Among the 170 unconnected ponds inventoried in the 2008 satellite imagery (Salerno et al., 2012) in  
293 the SNP, we tracked, according to the criteria described above, a total of 64 ponds (approximately 1/3)  
294 (Fig. 2a). Table 2 provides a general summary of their morphological features. We use the median values  
295 to describe these water bodies because, in general, we observed that these morphological data do not  
296 follow a normal distribution. The population consists of ponds larger than approximately 1 hectare ( $1.1$   
297  $10^4$  m<sup>2</sup>), located on relatively steep slopes ( $27^\circ$ ), and mainly oriented towards south-southeast ( $159^\circ$ ).  
298 These ponds are located at a median elevation of 5181 m a.s.l. and within an elevation zone ranging from  
299 4460 to 5484 m a.s.l..The observed changes in the surface area of all the considered ponds are listed in  
300 Table 3. In general, all unconnected ponds decreased by approximately  $10\pm 5\%$  in surface area in the last  
301 fifty years (1963-2013), with a significant difference based on the Friedman test ( $p < 0.01$ ). Figure 4d and  
302 Table 3 show that, until the 2000s, the ponds had a slight but not significant increasing trend ( $+7\pm 4\%$ ,  
303  $p > 0.05$ ). Since 2000, they have decreased significantly ( $-1.7\pm 0.6\%$  yr<sup>-1</sup>,  $p < 0.001$  corresponding to -  
304  $22\pm 18\%$ ).

305 As for glaciers, Figure 4c reports the glacier surface area changes observed across the SNP  
306 (approximately 400 km<sup>2</sup>) observed by Thakuri et al., 2014. They reported a decrease of  $-13\pm 3\%$  from  
307 1963 to 2011. We updated this series to 2013 and found loss of surface area of  $-18\pm 3\%$ . For the glaciers  
308 located in the basins containing the considered ponds, we tracked changes little bit larger. Their overall  
309 surface was 32.2 km<sup>2</sup> in 1963 and 25.0 km<sup>2</sup> in 2013, with a decrease of  $-26\pm 20\%$  (Fig. 4c; Table 3).  
310 According to many authors (e.g., Loibl et al., 2014), as we observe here, the main losses in area over the  
311 last decades in the Himalaya have been observed in smaller glaciers.

## 312 5. Discussion

313 **5.1 Short-term inter-annual analysis: investigation on potential drivers of change** Considering the  
314 wide availability of satellite imagery during the 2000-2013 period, an inter-annual analysis has been  
315 carried on 10 selected ponds in order to investigate the possible drivers of change. This was made  
316 possible exploiting the continuous series of annual pond surface areas on the one side, and climatic data  
317 from Pyramid station on the other.

### 318 5.1.1 Trends in pond surface areas

319 Table 4 provides the morphometric characteristics of 10 selected ponds. We observe that the median  
320 features of these ponds are comparable with the entire pond population (Table 2), highlighting the good  
321 representativeness of the selected case studies. Figure SI2 shows, for each pond, the annual surface area  
322 variations that occurred during the 2000-2013 period. All the selected ponds show a significant ( $p < 0.05$ )  
323 decreasing trend according to what has been observed for the whole pond population during the same  
324 period.

### 325 5.1.2 Trends in possible drivers of change

326 The selected possible drivers of change are: temperature (daily maximum, minimum and mean),  
327 precipitation, potential evaporation, and glacier melt of the pre-monsoon, monsoon (Fig. 5), and post-  
328 monsoon seasons. Pyramid data have been used for computing or aggregating these variables. The  
329 assumption behind this analysis is that these series can be considered representative both along the

330 altitudinal gradient and in the different valleys of the SNP. The scarcity of land weather data at these  
331 elevations makes licit this assumption, although, at this regard, the detected drivers of change will be  
332 analyzed in this respect in the last paragraph.

333 All these trends are noted in Figure SI3, and a correlation table comparing pond surface area variations  
334 and potential drivers of change is presented in Table SI5. In general, we observe from this table that the  
335 highest correlations are found for the monsoon period. The reason is because 90% of the precipitation and  
336 the highest temperatures are recorded during this period (Salerno et al., 2015). Consequently, the main  
337 hydrological processes in the Himalaya occur during the monsoon season. Focusing on this season, we  
338 first observe from Figure SI3 a large and significant precipitation decrease ( $-11 \text{ mm yr}^{-1}$ ;  $p<0.1$ ). Even the  
339 mean temperature decreases, but slightly and not significantly. This is a result of a significant decrease in  
340 maximum temperature ( $-0.08 \text{ }^\circ\text{C yr}^{-1}$ ;  $p<0.05$ ) balanced by an increase in minimum temperature. The  
341 potential evaporation, calculated on the basis of the mean temperature and global radiation, is constant  
342 during the summer period. These trends have been more broadly discussed in Salerno et al., 2015. They  
343 observed, for a longer period (since 1994), that the mean air temperature has increased by  $0.9 \text{ }^\circ\text{C}$  ( $p<0.05$ )  
344 at the annual level. However, the warming has occurred mainly outside the monsoon period and mainly in  
345 the minimum temperatures. Moreover, as we observed here for the 2000-2013 period, a decrease in  
346 maximum temperature from June to August ( $-0.05 \text{ }^\circ\text{C yr}^{-1}$ ,  $p<0.1$ ) has been observed. In terms of  
347 precipitation, a substantial reduction during the monsoon season (47%,  $p<0.05$ ) has been observed.

348 The glacier melt related to each glacier within the pond basins has been calculated considering both  
349 maximum and mean daily temperature. The averages for all selected cases are analyzed for each season in  
350 Figure SI3, which reveals that the only period producing a sensible contribution is the monsoon period if  
351 the maximum daily temperatures are considered the main driver of the process. The reason can be easily  
352 observed in Figure 2b, which shows the  $0 \text{ }^\circ\text{C}$  isotherms corresponding to the mean and maximum  
353 temperatures. Only the  $0 \text{ }^\circ\text{C}$  isotherm related to the daily maximum temperature during the monsoon  
354 period is located higher than the mean elevation of the analyzed glaciers. The T-index model only  
355 calculates the melting associated with temperatures above  $0 \text{ }^\circ\text{C}$ , thereby explaining this pattern. In other  
356 words, the diurnal temperatures influence the melting processes much more than the nocturnal ones,  
357 which are considered in the mean daily temperature. Figure 6b shows that the trend is significantly  
358 decreasing ( $3\% \text{ yr}^{-1}$ ,  $p<0.05$ ), according to the decrease observed in maximum temperature.

### 359 5.1.3 Detection of drivers of change

360 As anticipated, the highest correlations pond surface areas are found for the monsoon period. Based  
361 on Table SI5, we observe that precipitation, maximum temperature, and glacier melt (calculated from  
362 temperature) are the more correlated variables. The PCA shown in Figure 5 attempts to provide an  
363 overall overview of the relationships, during the monsoon period, among the trends related to the  
364 potential drivers of change and the pond surface areas. This representation helps to further summarize the  
365 main components of the water balance system that influence the pond surface areas, i.e., glacier melt and  
366 precipitation. We observe that evaporation is not an important factor at these elevation and that the  
367 evaporation/precipitation ratio is approximately 0.41. Therefore, a hypothetical variation in the  
368 precipitation regime affects the pond water balance two and half times more than the same variation in the  
369 evaporation rate. Moreover, from Figure 5, we observe that there are some ponds that are more correlated  
370 with the monsoon precipitation (i.e., LCN76, LCN141, LCN77, LCN11, and LCN93) and others that are  
371 more correlated with the glacier melt (i.e., LCN68, LCN3, and LCN9). A few ponds seem influenced by  
372 both drivers (i.e., LCN24 and LCN139). The coefficients of correlation are reported in Table 4. According

373 to the grouping observed with the PCA.

374 Figure 6 shows good fits between the pond surface area trends and the main drivers of change. Based  
375 on Table 4, ponds with higher glacier coverage within the basin show higher correlations with the glacier  
376 melt, and, in contrast, ponds with lower glacier coverage show higher correlations with precipitation, i.e.,  
377 the glacier coverage is the discriminant variable. In our case study, the threshold between the two groups  
378 appears to be a glacier coverage of 10%.

## 379 **5.2 Long-term inter-annual analysis**

380 An inter-annual analysis has been carried out from 1963 to 2013 on all 64 considered pond in order to  
381 investigate 1) which morphological boundary conditions control the pond surface area changes and 2) the  
382 capability of unconnected ponds to infer on the detected drivers of change also in the past when land  
383 climatic data did not exist.

### 384 **5.2.1 Morphological boundary conditions controlling the pond surface area changes**

385 We analyzed whether all 64 considered ponds experienced changes in surface area in relation to  
386 certain morphological boundary conditions, such as the mean elevation of the basin, the pond surface  
387 area, the main three valleys of SNP (Fig. 2a), and the glacier cover. In this case, evaluated the normality  
388 of data, we apply the ANOVA test as well as the relevant post-hoc test described above. Figure SI4 shows  
389 the surface area changes observed during the 1992-2013 period vs morphological factors. The same  
390 analysis has been carried out also on 1963-1992 period reporting decidedly similar results (not shown  
391 here). We observe that the pond surface area changes are independent from both elevation, valley, and  
392 pond size, whereas significant differences can be observed between ponds with and without glacier cover.  
393 In particular, ponds-with-glaciers experienced a lower surface area reduction. This analysis reconfirms  
394 that the glacier cover at these altitudes is the main discriminant parameters in the hydrological cycle of  
395 unconnected ponds.

396 We now analysed whether ponds with and without glacier cover within their hydrological basin  
397 experienced changes in surface area in relation to the aspect and the elevation of the basin. The two  
398 classes have been defined accordingly to the observed threshold of 10%. Hereafter, we define these ponds  
399 as ponds without glaciers in the basin (ponds-without-glaciers), neglecting in this way relatively small  
400 glacier bodies, which could possibly be confused with snowfields. The opposite class is defined as ponds  
401 with glaciers in the basin (ponds-with-glaciers). Among ponds-with-glaciers, Table 2 shows that they are  
402 characterized by a median glacier coverage of 19%, oriented toward the east-southeast and relatively  
403 steep ( $31^\circ$ ). The observed changes according to this new classification are reported in Table 3.

404 In this analysis, we apply the Kruskal-Wallis test as the relevant post-hoc test described above. Figure  
405 7 shows the surface area changes observed during the 1992-2013 period. The changes were independent  
406 of both elevation and aspect for ponds-without-glaciers (Fig. 7a; Fig. 7c), whereas significant differences  
407 can be observed for ponds-with-glaciers. Ponds located at higher elevations experienced greater decreases  
408 (Fig. 7b). In particular, ponds over 5400 m a.s.l. decreased significantly ( $p < 0.01$ ) more than ponds located  
409 below 5100 m a.s.l. In terms of aspect, the south-oriented ponds (Fig. 7d) experienced greater decreases,  
410 which was significantly different from southeast ( $p < 0.01$ ) and southwest ( $p < 0.01$ ) orientations.

411 The tracking of pond surface area provides important information on precipitation and glacier melt  
412 trends in space. Ponds-without-glaciers allows to understand that the precipitation in the SNP generally  
413 occur homogeneously at all elevations and in all valleys independent of the orientation (Fig. 7a; Fig. 7c).  
414 Based on the greater loss of surface area for ponds-with-glaciers at lower elevations, we can infer that

415 glacier melt is actually higher at these elevations, surely due to the effect of higher temperatures (Fig. 7b).  
416 Even in valleys oriented in directions other than south, we observe greater losses in surface area for  
417 ponds-with-glaciers (Fig. 7d). Small glaciers lying in perpendicular valleys, which are much steeper than  
418 the north-south-oriented valleys (following the monsoon direction), are likely melting more due to their  
419 small size and higher gravitational stresses (e.g., Bolch et al., 2008; Quincey et al., 2009).

## 420 **5.2.2 Pond surface areas as proxy of past changes of the hydrological cycle**

### 421 **Climate reconstruction**

422 To reconstruct the climatic trends before 1994, we compared the annual and seasonal precipitation and  
423 temperature time series recorded at Pyramid station since 1994 (Salerno et al., 2015) with selected  
424 regional gridded and reanalysis datasets (Table SI1). Table 1 shows the coefficient of correlation found  
425 for these comparisons. Era Interim ( $r = 0.92$ ,  $p < 0.001$ ) for mean temperature (Fig. 4a) and GPCC ( $r =$   
426  $0.92$ ,  $p < 0.001$ ) for precipitation (Fig. 4b) provide the best performance at the annual level. Figure SI5  
427 shows the location of Era Interim and GPCC nodes close to the region of investigation and in particular in  
428 relation to the Pyramid station. The comparisons between gridded/reanalysis and land data are visualized  
429 in Figure SI6. We observe that precipitation increased significantly until the middle 1990s (+25.6%,  $p <$   
430  $0.05$ , 1970-1995 period), then it started to decrease significantly (-23.9%,  $p < 0.01$ , 1996-2010 period), as  
431 observed by the Pyramid station and described by Salerno et al., 2015. The mean temperature reveals a  
432 continuous increasing trend ( $+0.039$  °C yr<sup>-1</sup>,  $p < 0.001$ , 1979-2013 period) that has accelerated since the  
433 early of 1990s.

434 Furthermore, Table 1 shows the low capability of all the products to correctly simulate monsoon  
435 temperatures and in particular the daily maximum ones. Figure SI7a reports visually the correlations at  
436 monthly level for maximum temperature, while Figure SI7b highlights the misfit in the time between the  
437 maximum, mean, and minimum temperature trends during the monsoon period.

### 438 **Analysis of ponds surface area in the last fifty years**

439 The maps in Figure 8 show the spatial differences between the two pond classes and compare the  
440 relative annual rate of change. Generally, no difference can be observed at valley level, as confirmed by  
441 the test applied above (Fig. SI4). It is interesting to visually observe most of the pond-without-glaciers  
442 increased in the 1963-1992 period, while pond-with-glaciers increased in the 1992-2000 period. Almost  
443 all the considered ponds decreased during 2000-2013 period.

444 Figure 9 tracks their trends over time. We have already discussed (Fig. 4d) that, in general, all  
445 unconnected ponds over the last fifty years have decreased by approximately 10%. Additionally, the  
446 presence of glaciers within the pond basins results in divergent trends. The surface area of ponds-without-  
447 glaciers strongly decreased ( $-25 \pm 6\%$ ,  $p < 0.001$ ), from 1963 to 2013 (Fig. 9a). In contrast, the surface area  
448 of ponds-with-glaciers decreased much less ( $-6 \pm 2\%$ ,  $p < 0.05$ ) for the same period (Fig. 9b). Differences in  
449 behavior are also noticeable among the periods pointed out in Table 3. In this case, we compare the  
450 median values of the relative annual rates of change. From 1963 to 1992, ponds-without-glaciers  
451 increased slightly ( $0.9 \pm 0.5\%$  yr<sup>-1</sup>,  $p < 0.1$ ), whereas the other ones remained constant ( $0.0 \pm 0.1\%$  yr<sup>-1</sup>).  
452 From 1992 to 2000, ponds-without-glaciers decreased slightly ( $-1.1 \pm 1.9\%$  yr<sup>-1</sup>,  $p > 0.1$ ), whereas the other  
453 ones increased slightly but significantly ( $+0.7 \pm 0.5\%$  yr<sup>-1</sup>,  $p < 0.05$ ). In the most recent period (2000 to  
454 2013), both categories decreased, but ponds-without-glaciers decreased more ( $-2.3 \pm 0.7\%$  yr<sup>-1</sup>,  $p < 0.001$ ;  $-$   
455  $1.5 \pm 0.4\%$  yr<sup>-1</sup>,  $p < 0.001$ ).

456 The significance of the divergent trend observed between the two groups has been tested for two  
457 periods (1963-1992 and 1992-2013). Based on a Kruskal-Wallis test, in the first period, ponds-without-  
458 glaciers presented significantly ( $p < 0.01$ ) higher increases than ponds-with-glaciers ( $+13 \pm 12\%$ ;  $0 \pm 3\%$ ,  
459 respectively). Differently, in the second period ponds-without-glaciers shown higher and significantly  
460 ( $p < 0.01$ ) decreases ( $-38 \pm 6\%$ ;  $-6 \pm 2\%$ , respectively).

461 Focusing the attention on Figure 9, this analysis concludes by assessing what we have learned from  
462 pond surface areas for the last fifty years. An increase in precipitation occurred until the middle 1990s  
463 followed by a decrease until recent years. This is shown observing the GPCP precipitation series, but it is  
464 also confirmed by the behavior of ponds-without-glaciers (Fig. 9a). With regard to the glacier melt, until  
465 the 1990s it was constant. Then, an increase occurred in the early 2000s, while in the recent years a  
466 declining was observed (Fig. 9b). This is the trend shown by ponds-with-glaciers. Furthermore, since  
467 1994 the glacier melt, calculated directly from the maximum temperature, which has been recorded by the  
468 Pyramid Laboratory, is fully in agreement with the behavior of ponds-with-glaciers. Before 1994 suitable  
469 maximum temperature cannot be derived from Gridded and Reanalysis products (Table 1 and Fig. SI7),  
470 but the ponds are able to point out that the glacier melt in those years has been constant. Simply tracking  
471 the glacier surface areas did not yield information on the temporal behavior of glacier melt. A decrease in  
472 glacier surface area has been identified over the last fifty years (Fig. 4c), but this reduction does not  
473 correspond to an increase in glacier melt, as normally expected. As discussed by other authors (Thakuri et  
474 al., 2014; Salerno et al., 2015; Wagnon et al., 2013), on the south slopes of Mt. Everest, the weaker  
475 precipitation could be the main cause of glacier shrinkage. In recent years, glaciers are accumulating less  
476 than they were decades ago; thus, their size is declining. In contrast, the tracking of pond surface areas  
477 demonstrates that glacier melt did not have a trend congruent to the glacier shrinkage being influence  
478 more to the maximum temperature trend.

## 479 **6. Conclusion**

480 The main contribution provided by this study is to have demonstrated for our case study that surface  
481 areas of unconnected ponds could be tracked to detect the behavior of precipitation and glacier melt in  
482 remote and barely accessible regions where, even for recent decades, few or no time series exist. Local  
483 end peculiar morphological conditions of each pond (possibly enhanced or reduced sediment supply,  
484 landslides, groundwater, etc...) could influence the pond surface area. However, the significant  
485 relationships found here on a wide pond population demonstrate that these factors are secondary  
486 respect to the main components of the hydrological cycle.

487 In high-elevation Himalayan areas, unconnected glacial ponds have demonstrated a high sensitivity to  
488 climate change. In general, over the last fifty years (1963-2013), unconnected ponds have decreased  
489 significantly by approximately  $10 \pm 5\%$ . We attribute this change to both a drop in precipitation and a  
490 decrease in glacier melt caused by a decline in the maximum temperature in the recent years. Evaporation  
491 has little effect at these elevations and has remained constant over the last decade, during which the main  
492 decline in ponds surface area has been observed.

493 An increase in precipitation occurred until the middle 1990s followed by a decrease until recently.  
494 With regard to the glacier melt, until the 1990s it was constant. Then, an increase occurred in the early  
495 2000s, while in the recent years a declining. Simply tracking the glacier surface areas did not yield  
496 information on the temporal behavior of glacier melt. A decrease in glacier surface area has been  
497 identified over the last fifty years, attributed by other authors to mainly the observed weaker precipitation.  
498 In contrast, the tracking of pond surface areas demonstrates that glacier melt did not have a trend

499 congruent to the glacier shrinkage being chiefly influenced by the maximum temperature trend.

500 In conclusion, a question arises in regard to the portability of this method. Here, portability refers to  
501 the degree to which the proposed method is replicable in other remote environments. In the Himalaya,  
502 other land based climatic series at high elevations are decidedly scarce (Barry, 2012; Rangwala and  
503 Miller, 2012; Pepin et al., 2015; Salerno et al., 2015). The inferences developed here could be simply  
504 applied and trends in precipitation and glacier melt inferred for the overall mountain range. Observing  
505 differences in the magnitude of changes between the two classes that differ in glacier coverage (threshold  
506 of 10%) across different periods, along an elevation gradient, or according to the basin aspect, as carried  
507 out here, could improve the confidence of the inferred findings. In contrast, in other mountain ranges with  
508 other climatic conditions, the inferences developed here might not be valid, and station-observed climatic  
509 data would be required to test the ability of glacier ponds to detect the main water balance components.

510

#### 511 **Author contributions**

512 F.S. and G.T. designed research; F.S. N.G. and S.T. analyzed data; F.S. wrote the paper. F.S. N.G. S.T.  
513 G.V. and G.T. check the data quality.

#### 514 **Acknowledgements**

515 This work was supported by the MIUR through Ev-K2-CNR/SHARE and CNR-DTA/NEXTDATA  
516 project within the framework of the Ev-K2-CNR and Nepal Academy of Science and Technology  
517 (NAST).**References**

- 518 Adrian, R., O'Reilly, C. M., Zagarese, H., Baines, S.B., Hessen, D.O., Keller, W., Livingstone, D. M.,  
519 Sommaruga, R., Straile, D., van Donk, E., Weyhenmeyer, G. A., and Winderl, M.: Lakes as sentinels  
520 of climate change, *Limnol. Oceanogr.*, 54, 2283–2297, doi:10.4319/lo.2009.54.6\_part\_2.2283, 2009.
- 521 Ageta, Y. and Fujita, K.: Characteristics of mass balance of summeraccumulation type glaciers in the  
522 Himalayas and Tibetan Plateau, *Z. Gletscherkd, Glazialgeol.*, 32, 61–65, 1996
- 523 Ageta, Y., Iwata, S., Yabuki, H., Naito, N., Sakai, A., Narama, C., and Karma, T.: Expansion of glacier  
524 lakes in recent decades in the Bhutan Himalayas, *IAHS Publication*, 264, 165–175, 2000.
- 525 Amatya, L. K., Cuccillato, E., Haack, B., Shadie, P., Sattar, N., Bajracharya, B., Shrestha, B. Caroli, P.,  
526 Panzeri, D., Basani, M., Schommer, B., Flury, B. Salerno, F., and Manfredi, E. C.: Improving  
527 communication for management of social-ecological systems in high mountain areas: Development of  
528 methodologies and tools – The HKKH Partnership Project, *Mt. Res. Dev.*, 30, 69-79,  
529 doi:10.1659/MRD-JOURNAL-D-09-00084.1, 2010.
- 530 Bajracharya B., Uddin, K., Chettri, N., Shrestha, B., and Siddiqui, S. A.: Understanding land cover  
531 change using a harmonized classification system in the Himalayas: A case study from Sagarmatha  
532 National Park, Nepal, *Mt. Res. Dev.*, 30, 143–156, doi: 10.1659/MRD-JOURNAL-D-09-00044.1,  
533 2010.
- 534 Barry, R. G.: Recent advances in mountain climate research, *Theor. Appl. Climatol.*, 110, 549-553,  
535 doi:10.1007/s00704-012-0695-x, 2012.
- 536 Benn, D., Wiseman, S., and Hands, K.: Growth and drainage of supraglacial lakes on debris mantled  
537 Ngozumpa Glacier, Khumbu Himal, Nepal, *J. Glaciol.*, 47 (159), 626-638,  
538 doi:http://dx.doi.org/10.3189/172756501781831729, 2001.
- 539 Bhujju, D. R., Carrer, M., Gaire, N. P., Soraruf, L., Riondato, R., Salerno, F., and Maharjan, S. R.: Den-  
540 droecological study of high altitude forest at Sagarmatha National Park, Nepal, in: *Contemporary Re-*  
541 *search in Sagarmatha (Mt. Everest) Region, Nepal: An Anthology*, edited by: Jha, P. K. and Khanal, I.  
542 P., Nepal Academy of Science and Technology, Kathmandu, Nepal, 119–130, 2010.
- 543 Bolch, T., Buchroithner, M., Pieczonka, T., and Kunert, A.: Planimetric and volumetric glacier changes in  
544 the Khumbu Himal, Nepal, since 1962 using Corona, Landsat TM and ASTER data, *J. Glaciol.*, 54,  
545 592–600, doi: 10.3189/002214308786570782, 2008.

546 Bolch, T., Kulkarni, A., Kääb, A., Huggel, C., Paul, F., Cogley, J. G., Frey, H., Kargel, J. S., Fujita, K.,  
547 Scheel, M., Bajracharya, S., and Stoffel, M.: The state and fate of Himalayan glaciers, *Science*, 336,  
548 310–314, 2012

549 Bolch, T., Pieczonka, T., and Benn, D. I.: Multi-decadal mass loss of glaciers in the Everest area (Nepal  
550 Himalaya) derived from stereo imagery, *The Cryosphere*, 5, 349-358, doi:10.5194/tc-5- 349-2011,  
551 2011.

552 Fisher, N. I.: *Statistical Analysis of Circular Data*, Cambridge University Press, Cambridge, U.K., 1993.

553 Fox, J. and Weisberg, S.: *An R Companion to Applied Regression*, Second Edition, Sage, 2011. Frey, H.,  
554 Paul, F., and Strozzi, T.: Compilation of a glacier inventory for the western Himalayas from satellite  
555 data: methods, challenges and results, *Remote Sens. Environ.*, 124, 832–843, 2012

556 Fujita, K., Sakai, A., Nuimura, T., Yamaguchi, S., and Sharma, R.: Recent changes in Imja Glacial lake  
557 and its damming moraine in the Nepal Himalaya revealed by in situ surveys and multi-temporal  
558 ASTER imagery, *Environ. Res. Lett.*, 4, 1–7, doi: [http://dx.doi.org/10.1088/1748-](http://dx.doi.org/10.1088/1748-9326/4/4/045205)  
559 2009.

560 Gardelle, J., Arnaud, Y., and Berthier, E.: Contrasted evolution of glacial lakes along the Hindu Kush  
561 Himalaya mountain range between 1990 and 2009, *Global Planet. Change*, 75, 47–55, 2011.

562 Guyennon, N., Romano, E., Portoghesi, I., Salerno, F., Calmanti, S., Petrangeli, A. B., Tartari, G., and  
563 Copetti, D.: Benefits from using combined dynamical-statistical downscaling approaches – lessons  
564 from a case study in the Mediterranean region, *Hydrol. Earth Syst. Sc.*, 17, 705–720,  
565 doi:10.5194/hess-17-705-2013, 2013

566 Hamerlik, L., Svitok, M., Novikmec, M., Ocadlík, M., and Bitušik, P.: Local among-site and regional  
567 diversity patterns of benthic macroinvertebrates in high altitude waterbodies: do ponds differ from  
568 lakes?, *Hydrobiologia*, doi: 10.1007/s10750-013-1621-7, 2013.

569 Hengl, T. and Reuter, H.: How accurate and usable is GDEM?, a statistical assessment of GDEM using  
570 LiDAR data, *Geomorphometry*, 2, 45–48, 2011.

571 Hervé, M.: *Diverse Basic Statistical and Graphical Functions (RVAideMemoire)*. R package, 2015.

572 Hock, R.: Temperature index melt modeling in mountain areas, *J. Hydrol.*, 282, 104-115, doi:  
573 10.1016/S0022-1694(03)00257-9, 2003.

574 Hothorn, T., Hornik K., van de Wiel, M. A., Wiel, H., and Zeileis, A.: *Conditional Inference Procedures*,  
575 R package, 2015.

576 Ichiyonagi, K., Yamanaka, M. D., Muraji, Y., and Vaidya, B. K.: Precipitation in Nepal between 1987  
577 and 1996, *Int. J. Climatol.*, 27, 1753–1762, doi:10.1002/joc.1492, 2007.

578 Jensen, M. E., and Haise, H. R.: Estimating evapotranspiration from solar radiation, *J. Irrig. Drain. Div.*,  
579 *Am. Soc. Civ. Eng.*, 89, 15–41, 1963.

580 Kääb, A., Berthier, E., Nuth, C., Gardelle, J., and Arnaud, Y.: Contrasting patterns of early twenty-first-  
581 century glacier mass change in the Himalayas, *Nature*, 488, 495–498, doi:10.1038/nclimate1580,  
582 2012.

583 Kayastha, R. B., Ageta, Y. and Nakawo M.: Positive degree-day factors for ablation on glaciers  
584 in the Nepalese Himalayas: Case study on Glacier AX010 in Shorong Himal, Nepal,  
585 *Bulletins of Glaciological Research*, 17, 1–10, 2000.

586 Kendall, M. G.: *Rank Correlation Methods*, Oxford University Press, New York, 1975.

587 Lami, A., Marchetto, A., Musazzi, S., Salerno, F., Tartari, G., Guilizzoni, P., Rogora, M., Tartari, G. A.:  
588 Chemical and biological response of two small lakes in the Khumbu Valley, Himalayas (Nepal) to  
589 short-term variability and climatic change as detected by long term monitoring and paleolimnological  
590 methods, *Hydrobiologia*, 648, 189–205, doi: 10.1007/s10750-010-0262-3, 2010.

591 LANDSAT SPPA Team: *IDEAS – LANDSAT Products Description Document*, Telespazio VEGA UK  
592 ([https://earth.esa.int/documents/10174/679851/LANDSAT\\_Products\\_Description\\_Document.pdf](https://earth.esa.int/documents/10174/679851/LANDSAT_Products_Description_Document.pdf)),  
593 2015.

594 Lei, Y., Yang, K., Wang, B., Sheng, Y., Bird, B. W., Zhang, G., and Tian, L.: Response of inland lake  
595 dynamics over the Tibetan Plateau to climate change, *Clim. Change*, 125, 281–290

596 doi:10.1007/s10584-014-1175-3, 2014.

597 Liu, Q., Mayer, C., and Liu S.: Distribution and interannual variability of supraglacial lakes on debris-  
598 covered glaciers in the Khan Tengri-Tomur Mountains, Central Asia, *Environ. Res. Lett.*, 10, 4545-  
599 4584, doi:10.5194/tcd-7-4545-2013, 2015.

600 Loibl, D. M., Lehmkuhl, F., and Grießinger, J.: Reconstructing glacier retreat since the Little Ice Age in  
601 SE Tibet by glacier mapping and equilibrium line altitude calculation, *Geomorphology*, 214, 22-  
602 39, doi: 10.1016/j.geomorph.2014.03.018, 2014.

603 Mann, H. B.: Nonparametric tests against trend, *Econometrica*, 13, 245-259, 1945.

604 Pepin N., Bradley R. S., Diaz H. F., Baraer M., Caceres E. B., Forsythe N., Fowler H., Greenword G.,  
605 Hashmi M. Z., Liu X. D., Miller J. D., Ning L., Ohmura A., Palazzi E., Rangwala I., Schonher W.,  
606 Severskiy I., Shahgedanova M., Wang M. B., Williamson S. N., and Yang D. Q.: Elevation-  
607 dependent warming in mountain regions of the world. *Nature Clim. Change*, 5(5), 424-430, doi:  
608 10.1038/nclimate2563, 2015.

609 Pham, S. V., Leavitt, P. R., McGowan, S., Peres-Nato, P.: Spatial variability of climate and land-use ef-  
610 fects on lakes of the northern Great Plains, *Limnol. Oceanogr.* 53, 728-742, doi:  
611 10.4319/lo.2008.53.2.0728, 2008.

612 Pohlert, T.: The Pairwise Multiple Comparison of Mean Ranks Package (PMCMR), R package. 2014.

613 Quincey, D. J., Luckman, A., and Benn, D.: Quantification of Everest region glacier velocities between  
614 1992 and 2002, using satellite radar interferometry and feature tracking, *J. Glaciol.*, 55, 596-606, doi:  
615 http://dx.doi.org/10.3189/002214309789470987, 2009.

616 Quincey, D., Richardson, S., Luckman, A., Lucas, R., Reynolds, J., Hambrey, M., and Glasser, N.: Early  
617 recognition of glacial lake hazards in the Himalaya using remote sensing datasets, *Global Plan.*  
618 *Change*, 56, 137-152, doi:10.1016/j.gloplacha.2006.07.013, 2007.

619 R Development Core Team. R: A language and environment for statistical computing. R Foundation for  
620 Statistical Computing, Vienna, Austria, ISBN 3-900051-07-0, URL <http://www.R-project.org>, 2008.

621 Rangwala, I., and Miller, J. R.: Climate change in mountains: a review of elevation-dependent warming  
622 and its possible causes, *Clim. Change*, 114, 527-547, doi: 10.1007/s10584-012-0419-3, 2012.

623 Razali, N. M., Waph, Y. B.: Power comparisons of Shapiro-Wilk, Kolmogorov-  
624 Smirnov, Lilliefors and Anderson-Darling tests, *J. Stat. Model. Anal.*, 2(1), 21-33,  
625 2011.

626 Pathak, P. and Whalen, S.: Using Geospatial Techniques to Analyse Landscape Factors  
627 Controlling Ionic Composition of Arctic Lakes, Toolik Lake Region, Alaska, in: *Geographic  
628 Information Systems: Concepts, Methodologies, Tools, and Applications*, edited by  
629 Information Resources Management Association, USA, Volume I, 130-150, doi:  
630 10.4018/978-1-4666-2038-4.ch012, 2013.

631 Reynolds, J.: On the formation of supraglacial lakes on debris-covered glaciers, *IAHS publication*, 264,  
632 153-161, doi: 10.3189/002214310791190785, 2000.

633 Sakai, A., and Fujita K.: Formation conditions of supraglacial lakes on debris covered glaciers in the  
634 Himalaya, *J. Glaciol.*, 56, 177-181, doi: 10.3189/002214310791190785, 2010.

635 Sakai, A.: Glacial lakes in the Himalayas: A review on formation and expansion processes, *Glob. Environ.*  
636 *Res.*, 16, 23-30, 2012.

637 Salerno, F., Cuccillato, E., Caroli, P., Bajracharya, B., Manfredi, E. C., Viviano, G., Thakuri, S., Flury, B.,  
638 Basani, M., Giannino, F., and Panzeri, D.: Experience with a hard and soft participatory modeling  
639 framework for social ecological system management in Mount Everest (Nepal) and K2 (Pakistan)  
640 protected areas, *Mt. Res. Dev.*, 30, 80-93, doi: <http://dx.doi.org/10.1659/MRD-JOURNAL-D-10-00014.1>, 2010.

641 Salerno, F., Gambelli, S., Viviano, G., Thakuri, S., Guyennon, N., D'Agata, C., Diolaiuti, G., Smiraglia,  
642 C., Stefani, F., Bochhiola, D., and Tartari, G.: High alpine ponds shift upwards as average temperature  
643 increase: A case study of the Ortles-Cevedale mountain group (Southern alps, Italy) over the last 50  
644 years, *Global Planet. Change*, doi: 10.1016/j.gloplacha.2014.06.003, 2014a. Salerno, F., Guyennon, N.,

645 Thakuri, S., Viviano, G., Romano, E., Vuillermoz, E., Cristofanelli, P., Stocchi, P., Agrillo, G., Ma,  
646 Y., and Tartari, G.: Weak precipitation, warm winters and springs impact glaciers of south slopes of  
647 Mt. Everest (central Himalaya) in the last 2 decades (1994–2013), *Cryosphere*, 9, 1229–1247,  
648 doi:10.5194/tc-9-1229-2015, 2015.

649 Salerno, F., Thakuri, S., D’Agata, C., Smiraglia, C., Manfredi, E. C., Viviano, G., and Tartari, G.: Glacial  
650 lake distribution in the Mount Everest region: Uncertainty of measurement and conditions of for-  
651 mation, *Global Planet. Change*, 92–93, 30–39, doi:10.1016/j.gloplacha.2012.04.001, 2012.

652 Salerno, F., Viviano, G., Carraro, E., Manfredi, E. C., Lami, A., Musazzi, S., Marchetto, A., Guyennon,  
653 N., Tartari, G., and Copetti, D.: Total phosphorus reference condition for subalpine lakes: comparison  
654 among traditional methods and a new process based and dynamic lake-basin approach, *J. Environ.*  
655 *Manag.*, 145, 94–105, doi:10.1016/j.jenvman.2014.06.011, 2014b.

656 Salerno, F., Viviano, G., Mangredi, E. C., Caroli, P., Thakuri, S., and Tartari, G.: Multiple Carrying Ca-  
657 pacities from a management-oriented perspective to operationalize sustainable tourism in protected  
658 area, *J. Environ. Manag.*, 128, 116–125, doi:10.1016/j.jenvman.2013.04.043, 2013.

659 Scherler, D., Bookhagen, B., and Strecker, M. R.: Spatially variable response of Himalayan glaciers to  
660 climate change affected by debris cover, *Nat. Geosci.*, 4, 156–159, 2011.

661 Settle, S., Goonetilleke, A., and Ayoko, G. A.: Determination of Surrogate Indicators for Phosphorus and  
662 Solids in Urban Storm water: Application of Multivariate Data Analysis Techniques, *Water Air Soil*  
663 *Poll.*, 182, 149–161, doi: 10.1007/s11270-006-9328-2, 2007.

664 Shapiro, S. S., and Wilk, M. B.: An analysis of variance test for normality (complete samples),  
665 *Biometrika*, 52, 591–611, 1965.

666 Smith, L. C., Sheng, Y., MacDonald, G. M., and Hinzman, L. D.: Disappearing Arctic Lakes, *Science*,  
667 308, 1429–1429, doi: 10.1126/science.1108142, 2005.

668 Smol, J. and Douglas, M.: From controversy to consensus: Making the case for recent climate change in  
669 the Arctic using lake sediments, *Front. Ecol. Environ.*, 5, 466–474, doi: 10.1890/060162, 2007.

670 Smol, J. P., Douglas, M. S. V.: Crossing the final ecological threshold in high Arctic ponds. *Proceedings*  
671 *of the National Academy of Sciences*, 104(30), 12395–12397, doi: 10.1073/pnas.0702777104, 2007.

672 Somos-Valenzuela, M. A., McKinney, D. C., Rounce, D. R., and Byers, A. C.: Changes in Imja Tsho in  
673 the Mount Everest region of Nepal, *Cryosphere* 8, 1661–1671., doi: 10.5194/tc-8-1661-2014, 2014.

674 Song, C., Huang, B., and Ke, L.: Heterogeneous change patterns of water level for inland lakes in High  
675 Mountain Asia derived from multi-mission satellite altimetry, *Hydrol. Process*, 29, 2769–2781, doi:  
676 10.1002/hyp.103992015, 2015.

677 Song, C., Huang, B., Richards, K., Ke, L., and Phan, V. H.: Accelerated lake expansion on the Tibetan  
678 Plateau in the 2000s: Induced by glacial melting or other processes?, *Water Resour. Res.*, 50(4), 3170–  
679 3186, doi: 10.1002/2013WR014724, 2014.

680 Tachikawa, T., Kaku, M., Iwasaki, A., Gesch, D., Oimoen, M., Zhang, Z., Danielson, J., Krieger, T., Cur-  
681 tis, B., Haase, J., Abrams, M., Crippen, R., and Carabajal, C.: ASTER Global Digital Elevation Model  
682 Version 2 – Summary of Validation Results, NASA Land Processes Distributed Active Archive Cen-  
683 ter and the Joint Japan-US ASTER Science Team  
684 ([https://lpdaacaster.cr.usgs.gov/GDEM/Summary\\_GDEM2\\_validation\\_report\\_final.pdf](https://lpdaacaster.cr.usgs.gov/GDEM/Summary_GDEM2_validation_report_final.pdf)), 2011.

685 Tartari, G., Previtali, L., and Tartari, G. A.: Genesis of the lake cadastre of Khumbu Himal Region  
686 (Sagarmatha National Park, East Nepal), in: *Limnology of high altitude lakes in the Mt Everest Re-*  
687 *gion (Nepal)*, edited by: Lami, A., and Giussani, G., *Mem. Ist. ital. Idrobiol.*, 57, 139–149, 1998.

688 Tartari, G., Salerno, F., Buraschi, E., Bruccoleri, G., and Smiraglia, C.: Lake surface area variations in the  
689 North-Eastern sector of Sagarmatha National Park (Nepal) at the end of the 20th Century by compari-  
690 son of historical maps, *J. Limnol.*, 67, 139–154, doi:10.4081/jlimnol.2008.139, 2008.

691 Thakuri, S., Salerno, F., Bolch, T., Guyennon, N., and Tartari, G.: Factors controlling the accelerated  
692 expansion of Imja Lake, Mount Everest region, Nepal, *Ann. Glaciol.*, 57, 245–257,  
693 doi:10.3189/2016AoG71A063, 2015.

694 Thakuri, S., Salerno, F., Smiraglia, C., Bolch, T., D’Agata, C., Viviano, G., and Tartari, G.: Tracing  
695 glacier changes since the 1960s on the south slope of Mt. Everest (central southern Himalaya) using

696 optical satellite imagery, *The Cryosphere*, 8, 1297-1315, doi:10.5194/tc-8-1297-2014, 2014.

697 Thompson, L. G., Thompson, E. M., Brecher, H., Davis, M., Leon, B., Les, D., Lin, P. N., Mashiotta, T.,  
698 and Mountain, K.: Abrupt tropical climate change: Past and present, *Proc. Natl. Acad. Sci. USA*, 103,  
699 10536–10543, 2006. Venables, W. N., and Ripley, B. D.: *Modern Applied Statistics with S*, Springer,  
700 New York, 2002.

701 Vuille, M.: Climate variability and high altitude temperature and precipitation, in: *Encyclopedia of snow,*  
702 *ice and glaciers*, edited by: Singh, V. P., Singh, P., and Haritashya, U. K., Springer, 153– 156, 2011.

703 Wagon, P., Vincent, C., Arnaud, Y., Berthier, E., Vuillermoz, E., Gruber, S., Ménégoz, M., Gilbert, A.,  
704 Dumont, M., Shea, J. M., Stumm, D., and Pokhrel, B. K.: Seasonal and annual mass balances of Mera  
705 and Pokalde glaciers (Nepal Himalaya) since 2007, *The Cryosphere*, 7, 1769–1786, doi:10.5194/tc-7-  
706 1769- 2013, 2013.

707 Wang, W., Xiang, Y., Gao, Y., Lu, A., and Yao, T.: Rapid expansion of glacial lakes caused by climate and  
708 glacier retreat in the Central Himalayas, *Hydrol. Process.*, 29, 859–874, doi:10.1002/hyp.10199, 2015.

709 Williamson, C. E., Dodds, W., Kratz, T. K., and Palmer, M.: Lakes and streams as sentinels of  
710 environmental change in terrestrial and atmospheric processes, *Front. Ecol. Environ.* 6, 247–254, doi:  
711 10.1890/070140, 2008.

712 Willmott, C. and Matsuura, K.: Advantages of the Mean Absolute Error (MAE) over the Root  
713 Mean Square Error (RMSE) in assessing average model performance, *Clim. Res.*, 30, 79–82,  
714 doi: 10.3354/cr030079, 2005.

715 Wold, S., Esbensen, K., and Geladi, P.: Principal component analysis. *Chemom. Intell. Lab.* 2, 37-52.  
716 1987.

717 Xie A., Ren, J., Qin, X., and Kang S.: Reliability of NCEP/NCAR reanalysis data in the  
718 Himalayas/Tibetan Plateau, *J. Geographical Sciences*, doi: 10.1007/s11442-007-0421-2, 2007.

719 Yao, T., Thompson, L., Yang, W., Yu, W., Gao, Y., Guo, X., Yang, X., Duan, K., Zhao, H., Xu, B., Pu J.,  
720 Lu A., Xiang Y., Kattel D. B., and Joswiak D.: Different glacier status with atmospheric circulations in  
721 Tibetan Plateau and surroundings, *Nat. Clim. Change*, 2, 663-667, doi: 10.1038/nclimate1580, 2012.

722 Zhang, G., Yao, T., Xie, H., Wang, W., and Yang, W.: An inventory of glacial lakes in the Third Pole  
723 region and their changes in response to global warming, *Glob. Planet. Change*, 131, 148–157,  
724 doi:10.1016/j.gloplacha.2015.05.013, 2015.

725

726

727

728

729

730

731

732

733

734

735

736 **Table 1.** Coefficients of correlation between precipitation and temperature time series recorded at  
 737 Pyramid station for the 1994-2013 period and gridded and reanalysis datasets (pre-monsoon, monsoon,  
 738 and post-monsoon seasons as the months of February to May, June to September, and October to January,  
 739 respectively). Bold values are significant with  $p < 0.01$ .

		APHRODIIE	GPCC	CRU	ERA Interim
Precipitation	annual	0.43	<b>0.75</b>	0.34	0.33
		NCEP CFS	GHCN	CRU	ERA Interim
Minimum Temperature	pre monsoon	<b>0.64</b>			<b>0.81</b>
	monsoon	0.47			<b>0.72</b>
	post monsoon	<b>0.70</b>			<b>0.65</b>
	annual	<b>0.72</b>			<b>0.92</b>
Mean Temperature	pre monsoon	<b>0.79</b>	<b>0.83</b>	<b>0.8</b>	<b>0.87</b>
	monsoon	0.61	0.51	0.42	<b>0.67</b>
	post monsoon	<b>0.79</b>	<b>0.77</b>	0.57	<b>0.82</b>
	annual	<b>0.81</b>	<b>0.85</b>	<b>0.89</b>	<b>0.92</b>
Maximum Temperature	pre monsoon	<b>0.83</b>			<b>0.88</b>
	monsoon	0.54			0.45
	post monsoon	<b>0.82</b>			<b>0.86</b>
	annual	<b>0.70</b>			<b>0.80</b>

740

741 **Table 2.** General summary of the morphological features of all 64 considered ponds (data from 2013).  
 742 Ponds are grouped according to the glacier cover present into each pond basin.

743

Topography	Glacier cover <10% median (range)	Glacier cover >10% median (range)	All lakes median (range)
Pond elevation (m a.s.l.)	5181(4460-5484)	5159(4505-5477)	5170(4460-5484)
Pond area ( $10^3 \text{ m}^2$ )	0.8(0.1-6.2)	1.3(0.3-56.3)	1.1(0.1-56.3)
Basin area ( $10^4 \text{ m}^2$ )	30(2-430)	130(30-2300)	70(2-2300)
Basin slope (°)	25(10-39)	29(23-41)	27(10-41)
Basin aspect (°)	163(68-256)	141(94-280)	159(68-280)
Basin mean elevation (m a.s.l.)	5293(4760-5531)	5400(5119-5945)	5315(4760-5945)
Basin/Pond area ratio ( $\text{m}^2/\text{m}^2$ )	60(3-485)	67(10-523)	64(3-523)
Glacier area (%)	0(0-9)	19(10-61)	0.5(0-61)
Glacier slope (°)	-	31(21-38)	-
Glacier aspect (°)	-	166(150-250)	-
Glacier mean elevation (m a.s.l.)	-	5680(5470-7500)	-

744

745

746

747

748

749

750 **Table 3.** General summary of surface area changes related to all 64 considered ponds from 1963 to 2013.  
 751 The surface area changes of the glaciers located within the basins are also reported. For each comparison  
 752 the uncertainty of measurement is also shown. On the right the cumulative loss respect to 1963 is reported  
 753 for eac intermediate period (these data are used for Fig. 8). On the left the relative annual rate are  
 754 calculated (these data are used for Fig. 7).

Period	Pond surface area change				Glacier surface area change	Period	Pond surface area change			
	Cumulative loss (%)		Cumulative loss (%)				Relative annual rate (% yr <sup>-1</sup> )			
Glacier coverage	< 10%	> 10%	All ponds	All basins	Glacier coverage	< 10%	> 10%	All ponds	All basins	
<b>1963-1992</b>	<b>+13±12</b>	<b>0 ±3</b>	<b>+3 ±7</b>	<b>8 ±8</b>	<b>1963-1992</b>	<b>0.9 ±0.5</b>	<b>0.0 ±0.1</b>	<b>+0.5 ±0.3</b>		
<b>1963-2000</b>	-1 ±6	+9 ±2 *	+7 ±4	-2 ±8	<b>1992-2000</b>	<b>-1.1 ±1.9</b>	<b>+0.7 ±0.5</b>	<b>-0.4 ±0.1</b>		
<b>1963-2008</b>	-4 ±5	+3 ±2	+1 ±4	-13 ±9 **	2000-2008	-0.3 ±1.0	-1.6±0.6	-0.7 ±0.7		
<b>1963-2011</b>	-7 ±6	0 ±2	-2 ±5	-14 ±14 **	2008-2011	0.0 ±2.8	0.0 ±1.6	0.0 ±2.2		
<b>1963-2013</b>	<b>-25 ±6 ***</b>	<b>-6 ±2 *</b>	<b>-10 ±5 **</b>	<b>-26 ±20 **</b>	2011-2013	-1.29 ±4.4 ***	-5.8 ±2.5 *	-1.4±3.5 **		
<b>1992-2013</b>	<b>-38 ±6 ***</b>	<b>-6 ±2 *</b>	<b>-13 ±5 **</b>	<b>-34 ±15 ***</b>	<b>2000-2013</b>	<b>-2.3±0.7 ***</b>	<b>-1.5 ±0.4 ***</b>	<b>-1.7 ±0.6 ***</b>		

755 *significance: p<0.001 '\*\*\*'; p<0.01 '\*\*'; p<0.05 '\*'; p<0.1 '\*'*

756 **Table 4.** Morphometric features of 10 selected ponds considered in the 2000-2013 analysis. Data are from  
 757 2013. Coefficients of correlation are for the monsoon season. The relationships with the other seasons are  
 758 reported in Table SI5.

Pond Code	Glacier Cover (%)	Pond Elevation (m a.s.l.)	Basin Aspect (°)	Basin Slope (°)	Basin Area (km <sup>2</sup> )	Pond Area (10 <sup>4</sup> m <sup>2</sup> )	Basin Elevation (m a.s.l.)	Coefficient of Correlation (Ponds surface area vs Precipitation)	Coefficient of Correlation (Ponds surface area vs Glacier melt)
LCN139	1	4749	75	30	0.6	4.6	5596	0.50	0.35
LCN93	2	5244	116	23	0.7	0.6	5502	0.70 **	0.39
LCN141	3	5316	152	27	1.4	2.6	5701	0.72 **	0.37
LCN11	3	5029	229	24	1.2	1.8	5372	0.76 **	0.49
LCN77	7	4920	142	26	8.6	18.3	5507	0.55 *	0.29
LCN76	9	4800	140	25	13.6	59.2	5457	0.65 **	0.23
LCN24	10	4466	162	28	23.0	54.0	5477	0.44	0.65 **
LCN9	13	5202	117	36	0.7	0.6	5792	-0.27	0.61 **
LCN3	30	5261	154	35	2.0	11.7	5981	0.17	0.87 ***
LCN68	32	5006	232	35	1.2	3.2	5686	0.12	0.65 **
<b>Median</b>	<b>8</b>	<b>5018</b>	<b>147</b>	<b>28</b>	<b>1.3</b>	<b>3.9</b>	<b>5551</b>		

759 *significance: p<0.001 '\*\*\*'; p<0.01 '\*\*'; p<0.05 '\*'; p<0.1 '\*'*

760

761

762

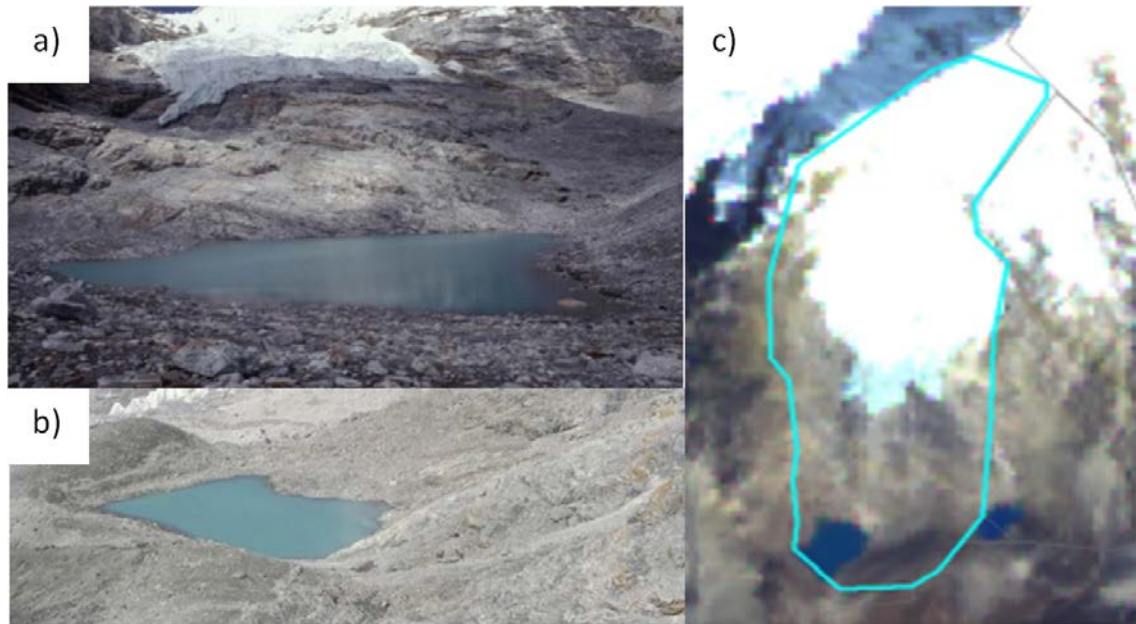
763

764

765

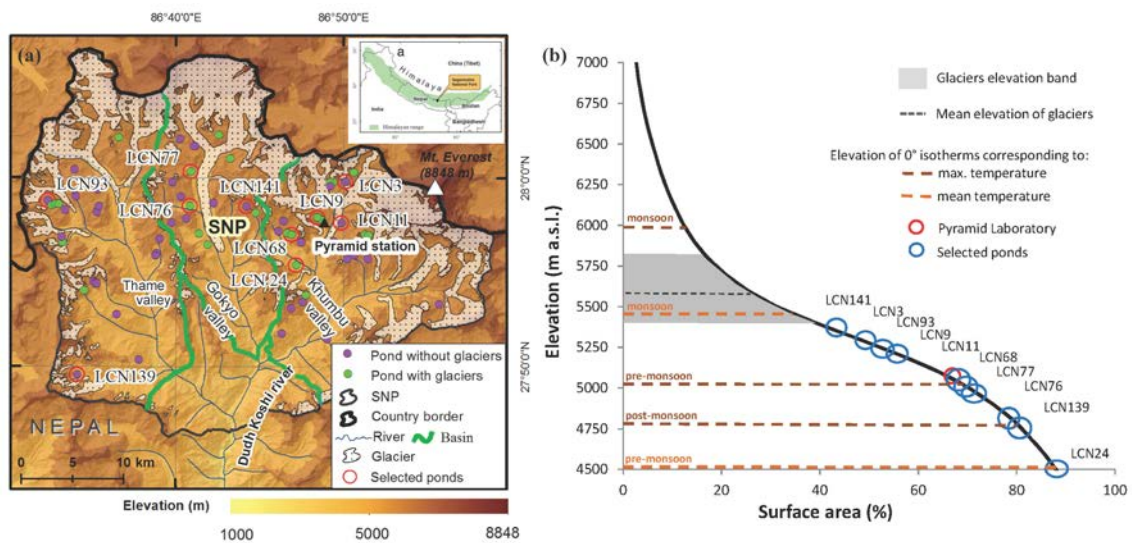
766

767



768

769 **Figure 1.** Example of an unconnected glacial pond (LCN5) with a glacier within the basin. Pictures were  
 770 taken in September 1992 (Gabriele Tartari): a) view looking north showing the distance between the  
 771 glacier and the pond surface; b) from east showing the frontal moraine. c) LCN5 basin tracked on ALOS  
 772 2008 imagery.



773

774

775

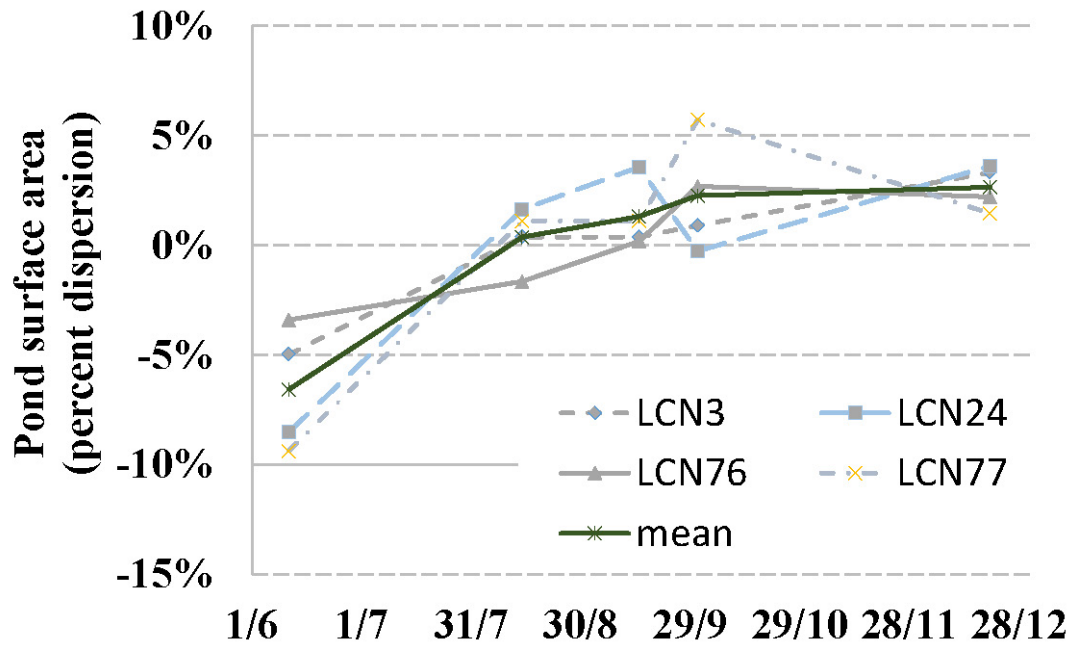
776

777

778

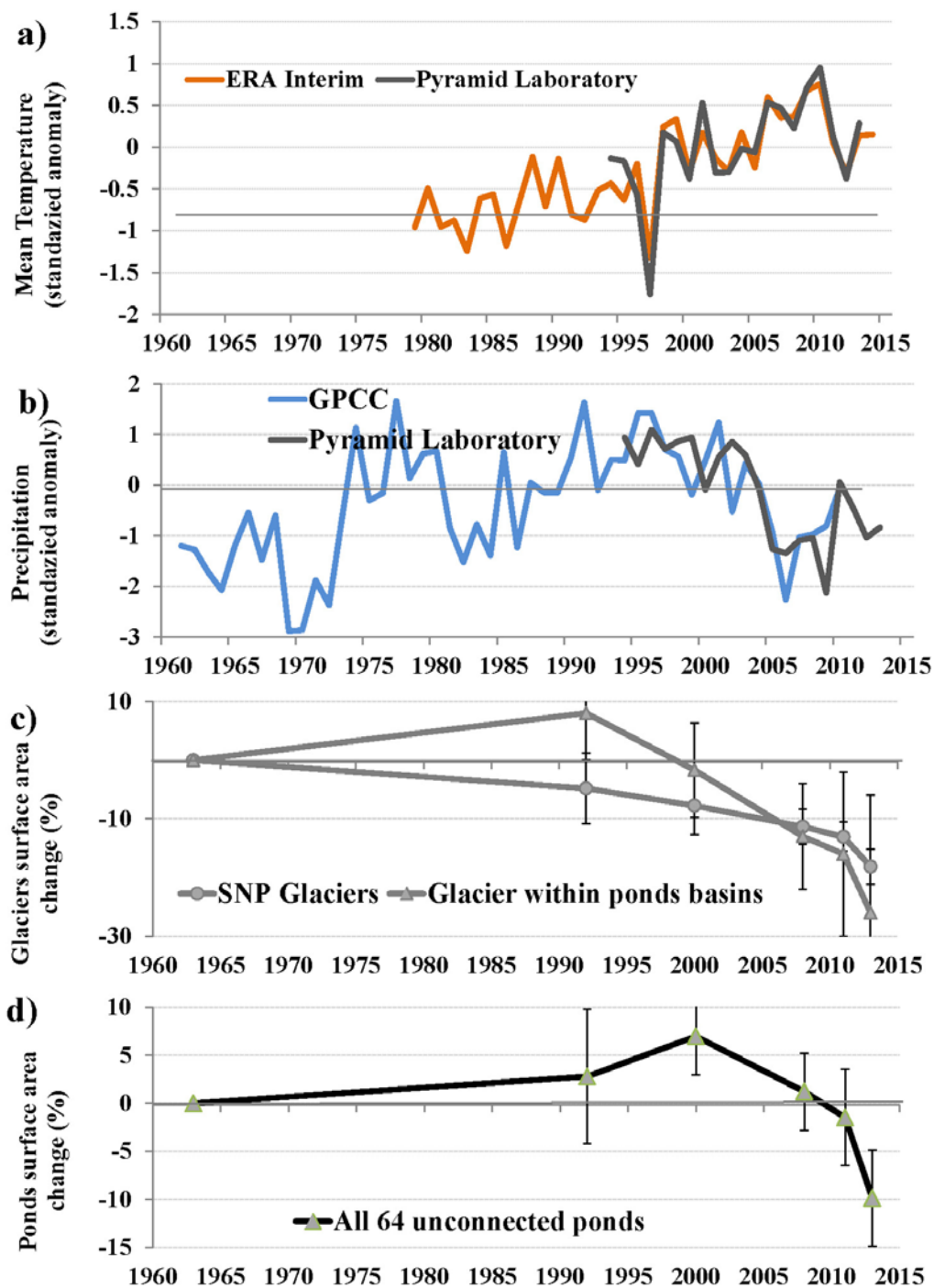
779

**Figure 2.** a) Location of the study area in the Himalaya and a detailed map of the spatial distribution of  
 all 64 unconnected ponds considered in this study. b) Hypsometric curve of SNP. Along this curve, the  
 locations of 10 selected ponds are shown. The 0 °C isotherms corresponding to the mean and maximum  
 temperature in 2013 are plotted for the pre-, post-, and monsoon period according to the lapse rates  
 reported in Salerno et al., 2015. The mean glacier elevation distribution (mean  $\pm$  1 standard deviation) of  
 10 selected ponds and the location of the Pyramid meteorological station are also reported.

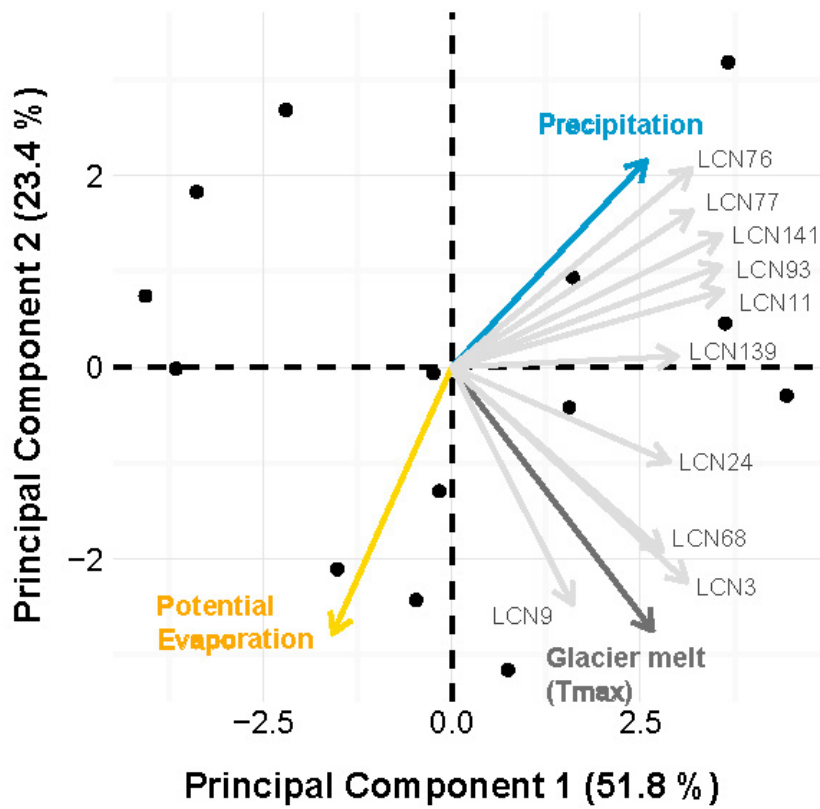


780  
781  
782

**Figure 3.** Intra-annual analysis (June-December) of selected pond surface areas. Percent dispersions are computed dividing the anomalies by the mean.



783  
784 **Figure 4.** Trend analysis of climate, glaciers and ponds surface area for the last fifty years in the SNP: a)  
785 Era Interim mean annual temperature compared with Pyramid’s land-based data; b) GPCP annual  
786 precipitation and Pyramid’s land-based data; c) Glacier surface area variations for the overall SNP  
787 (Thakuri et al., 2014) and for glaciers located in basins of 64 considered ponds. d) Surface area variations  
788 of all 64 considered ponds. Y-axis units: a) and b) Trends are expressed in terms of standardized  
789 anomalies divided by the standard deviation (dimensionless); c) and d) Relative variations with respect to  
790 1963. Errors bars represent the uncertainty of measurements.



791

792 **Figure 5.** Principal Component Analyses (PCAs) between pond surface area from 2000 to 2013 and  
 793 potential drivers of change (precipitation, glacier melt, and potential evaporation) related to the monsoon  
 794 season. Coefficients of correlation are reported in Table SI5. All trends related to ponds and variables are  
 795 provided in Figure SI5 and SI6.

796

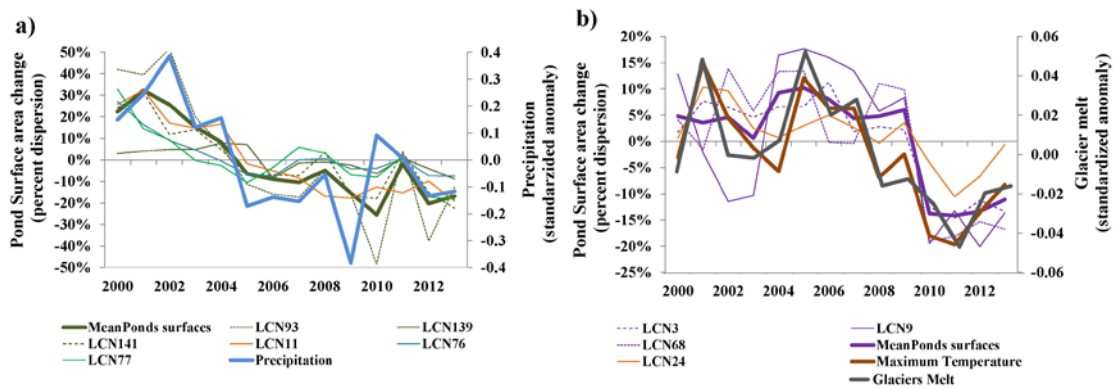
797

798

799

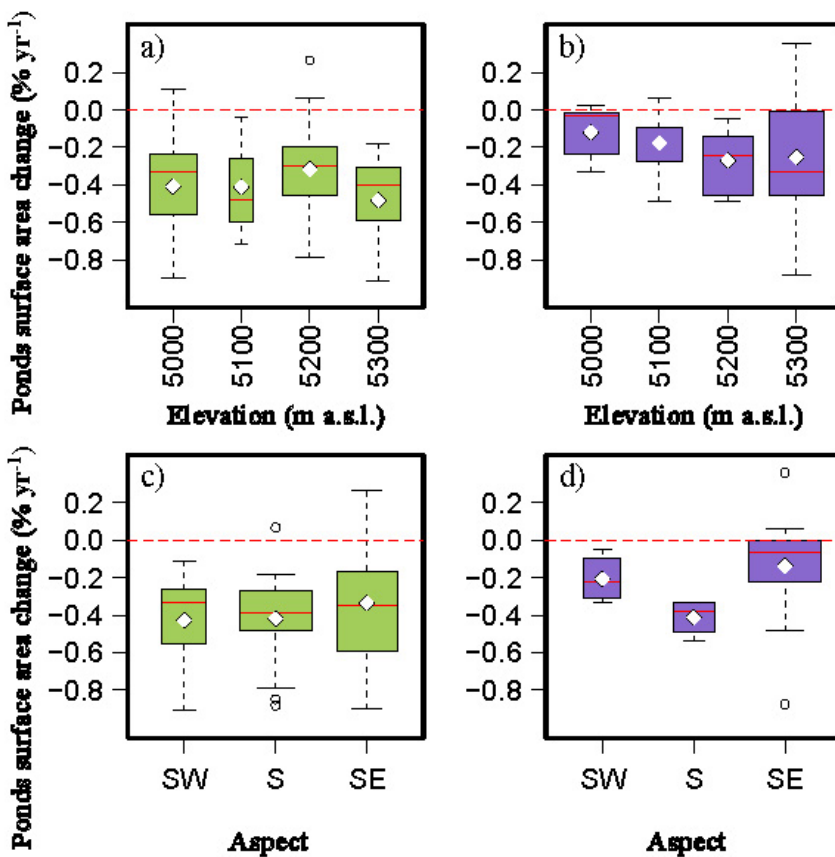
800

801



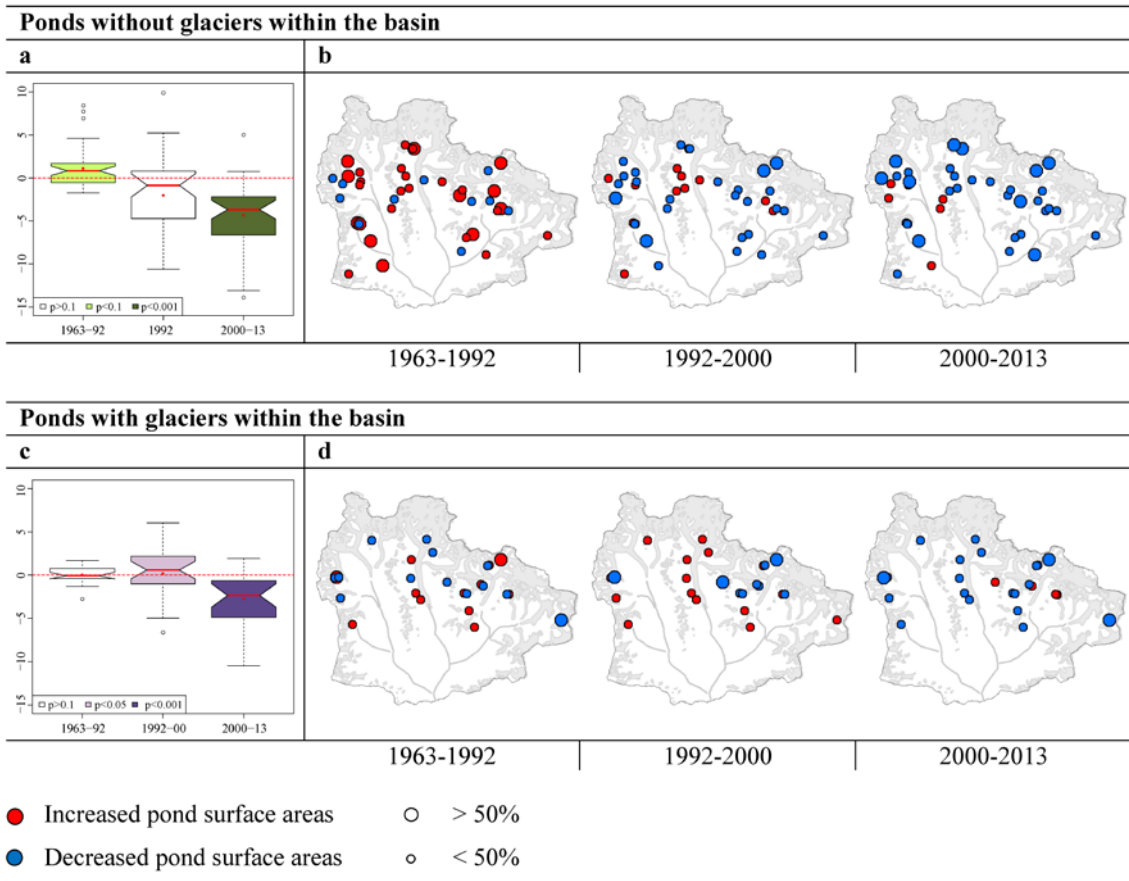
802

803 **Figure 6.** Annual trends from 2000 to 2013 related to pond surface area grouped according to the relevant  
 804 main drivers of change (monsoon season): a) precipitation, b) glacier melt . Coefficients of correlation are  
 805 reported in Table SI5. All trends related to ponds and variables are provided in Figures SI5 and SI6.  
 806 Standardized anomalies (dimensionless) are computed dividing the anomalies by the standard deviation.  
 807 Percent dispersions are computed dividing the anomalies by the mean.



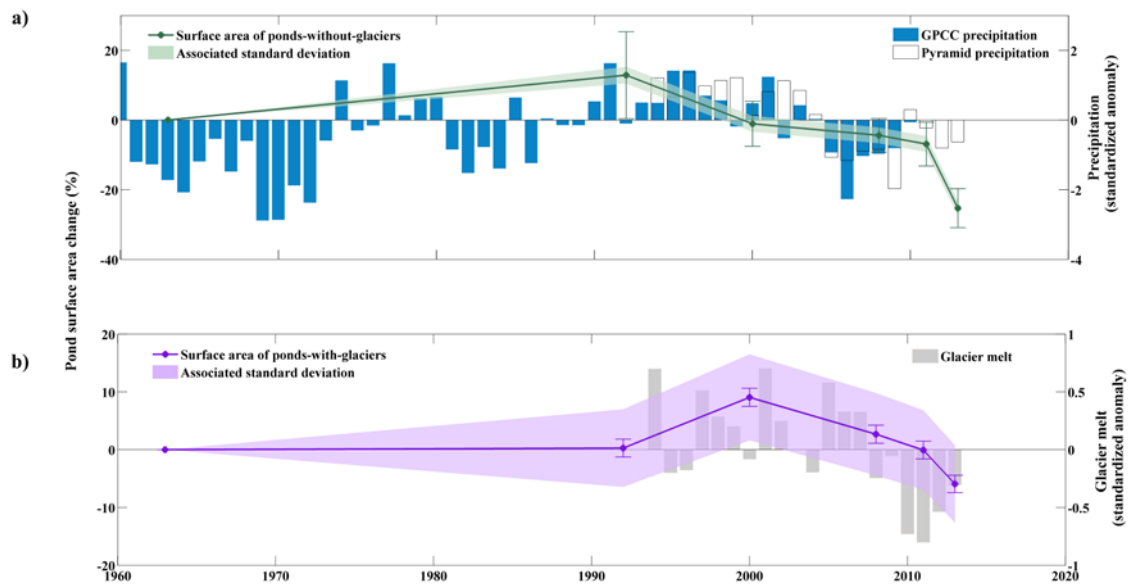
808

809 **Figure 7.** Pond surface area changes observed during the 1992-2013 period in relation to certain  
 810 morphological boundary conditions in the basin: elevation (upper graphs) and aspect (lower graphs). On  
 811 the left ponds-without-glaciers, and on the right ponds-with-glaciers. The white points in the boxplots  
 812 indicate the mean, whereas the red lines are the median.



813

814 **Figure 8.** Changes in pond surface area in the Mt. Everest region. The left boxplots represent the annual  
 815 rates of change of ponds in the analyzed periods: (a) ponds without glaciers within the basin, (c) ponds  
 816 with glaciers within the basin. The red points in the boxplots indicate the mean, whereas the red lines are  
 817 the median. Data are expressed as % yr<sup>-1</sup>. On the right side, the maps (b, d) visualize the variations that  
 818 occurred in the pond population during the same three periods considered in the relevant boxplots on the  
 819 left. Reference data are reported in Table 3. All percentages refer to the initial year of the analysis (1963).



820

821 **Figure 9.** Comparison for the last fifty years between the annual precipitation and the glacier melt with  
 822 the surface areas for a) ponds-without glaciers and b) ponds-with-glaciers. Standardized anomalies  
 823 (dimensionless) are computed dividing the anomalies by the standard deviation. Error bars represent the  
 824 uncertainty of measurements.